Semiclassical threshold law when the Wannier exponent diverges

P. Chocian, W. Ihra, and P. F. O'Mahony

Department of Mathematics, Royal Holloway, University of London, Egham, Surrey, TW20 0EX, United Kingdom

Using semiclassical methods we investigate the threshold behavior for three-particle breakup of a system with one particle of charge Z and two other particles of charge $-q$. For the particular case where the ratio of the charges of the third particle to the wing particles is $Z/q = 1/4$, the Wannier exponent for breakup diverges and the threshold law changes from a power law to an exponential law of the form $\exp(-\lambda/\sqrt{E})$. The threshold behavior is tested above the region of divergence and it is found that for $Z/q < 0.3$ a power law does not hold. Ionizing trajectories show that the dynamics within the near zone can become crucial to the energy dependence of the cross section. Cases are found to arise where more than one trajectory contributes to the same final state giving rise to semiclassical interference effects. [S1050-2947(98)05205-6]

PACS number(s): 34.80.Dp

I. INTRODUCTION

Wannier's picture of ridge propagation and Wannier theory [1] have been shown to give the correct threshold law when the cross section is calculated semiclassically for electron-impact ionization of hydrogen [2,3]. Near the threshold $E \to 0+$ Wannier theory predicts a power law
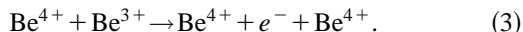
$$\sigma \sim E^\zeta \tag{1}$$

for the breakup cross section of three charged particles where E is the total energy of the system and ζ is the threshold exponent. In the case of a symmetric system where one of the particles has mass M and charge Z and the other two wing (outgoing) particles have equal masses m and charges $-q$ (Z and q have the same sign) one has for the exponent [4,5]

$$\zeta = \frac{3}{4}\sqrt{1 + \frac{16}{9}\frac{1+2m/M}{1-q/4Z} - \frac{1}{4}}. \tag{2}$$

If $m \ll M$, $q = 1$, and $Z = 1$, the original Wannier result $\zeta = 1.127$ is recovered for electron-impact ionization of hydrogen.

When the ratio of charges of the third particle to the wing particles is $Z/q = 1/4$, the Wannier exponent becomes infinite. This case arises in the process

$$Be^{4+} + Be^{3+} \to Be^{4+} + e^- + Be^{4+}. \tag{3}$$

We wish to find the semiclassical threshold law for this case and to test the validity of Wannier theory when Z/q is close to 1/4. In the following sections we study a model system of a nucleus of fractional charge Z and two electrons. When $Z = 1/4$ (atomic units used here and throughout) this system is analogous to the above case. The system is described within the semiclassical S-matrix formalism [2,3]. A threshold law of the form $\exp(-\lambda/\sqrt{E})$ is found to fit the cross section best; this is in agreement with the purely classical result of Dimitrijević *et al.* [6]. The functional form of the cross section is also in agreement with a recent analytical semiclassical prediction of Ihra *et al.* [7].

Cross sections are also calculated for a range of energies and nuclear charges and it is found that they do not follow a power law for a range of Z greater than 0.25, at least for energies greater than 0.01 eV. When $Z < 0.3$ the cross section does not fit a power law over the range of very low energies that we investigate.

In addition, deflection functions are found that are non-monotonic where different trajectories lead to the same final state and interfere in the semiclassical S matrix. This is a surprising result that differs from previous results for $Z = 1$ [3].

Ionizing trajectories that give a power law follow very similar paths in the reaction and Coulomb zones [1] for different small energies above threshold. These trajectories correspond to the orbits at small excess energy that Wannier showed are no different in these zones from orbits of zero energy. Ionizing trajectories that follow different paths within these zones (for the small energies used) give rise to a different law. The differing near-zone trajectories demonstrate the requirement that for certain systems the behavior in the near zone must be included to correctly evaluate the cross section.

II. THEORY

We use a semiclassical formulation for inelastic electron-atom scattering. It is derived from the path-integral representation of the S matrix and is especially designed to describe the threshold region of ionization [2,3].

In semiclassical S-matrix theory, for collisions near threshold ($E \to 0$), only the partial wave for total angular momentum $L = 0$ need be calculated. It is also sufficient to confine the system to a collinear configuration (an interelectronic angle of $\theta_{1,2} = 180°$, which is a fixed point of the classical equations of motion in a two-electron atom).

The relevant Hamiltonian for collinear two-electron motion is

$$H = \frac{p_1^2}{2} + \frac{p_2^2}{2} - \frac{Z}{r_1} - \frac{Z}{r_2} + \frac{1}{r_1+r_2}. \tag{4}$$

This Hamiltonian is regularized (see the Appendix) to remove the Coulomb singularities.

Semiclassical S-matrix theory incorporates two additional effects over Wannier's model. First, Wannier [1] assumed that points in phase space in the "reaction zone" are equally distributed. Semiclassical S-matrix theory drops this assumption and incorporates the behavior within this zone. Second, Wannier approximated the $\cos\theta_{1,2} = -1$ line across the saddle on the potential surface, in hyperspherical coordinates, as an inverted oscillator potential. Semiclassical S-matrix theory takes the exact line including singularities.

A. The semiclassical S matrix

Semiclassically, for this system the cross section reduces to a probability $P_{\varepsilon,\varepsilon'}$ that is directly proportional to the square modulus of the S matrix, given by

$$S_{\varepsilon,\varepsilon'}(E) = \sum_j \sqrt{\mathcal{P}(\varepsilon,\varepsilon')} \exp\left[\frac{i\Phi_j}{\hbar} - \frac{i\nu_j\pi}{2}\right]. \qquad (5)$$

The weight of the jth trajectory is determined by its probability

$$\mathcal{P}_j(\varepsilon,\varepsilon') = \frac{1}{R}\left|\frac{\partial\varepsilon}{\partial r_j'}\right|_{\varepsilon'}^{-1}, \qquad (6)$$

where R is the normalization constant, given by the sum of all processes that can happen, and r_j' is the initial position of the projectile on the jth trajectory. The classical action $\Phi_j(\varepsilon,\varepsilon') = \int q_1 dp_1 + \int q_2 dp_2$ and a contribution from the caustics and focal points along the trajectory (where the semiclassical approximation breaks down) of $\nu_j\pi/2$ define the accumulated phase of each trajectory. We sum over all classical trajectories j that take the projectile from initial energy ε' to final energy ε during the collision.

B. The classical deflection function

The position of the initial free electron r' (the "impact parameter") and its energy after collision ε (the "final-state observable") are used to describe ionization. The initial distance from the nucleus of the projectile is taken to be $r_0' + r'$, where r_0' is some arbitrary fixed distance large enough so that the result is independent of r_0' (4000 a.u. is suitable for the system we investigate) and r' is the parameter varied.

The deflection function (Fig. 1) is periodic in r' and has a period R' that is the distance that the asymptotically free projectile travels during a complete cycle on the Kepler ellipse of the bound electron. The parameter r' is varied over the distance R' and a deflection function is formed that represents all possible final states of the projectile electron. It now becomes apparent that for our particular choice of variables the normalization constant R that appears in Eq. (6) above takes the same value as R'.

It has been seen previously [2,3] that for the case where $Z=1$ the deflection function $\varepsilon(r')$ is found to be monotonic (it has only one intersection with a horizontal line at ε/E, indicating the correct initial condition r'), meaning that only a *single* trajectory contributes to each differential cross section with a final projectile energy ε. We find that whenever
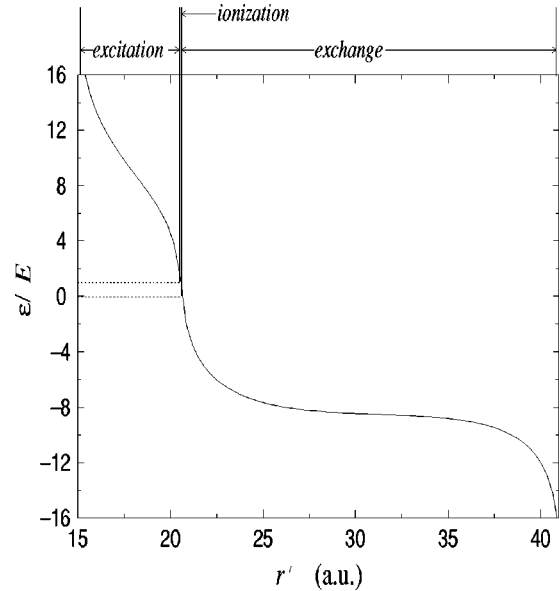

FIG. 1. Classical deflection function for final energy ε of the projectile electron as a function of its initial position 4000 a.u.$+r'$ for $Z=0.25$ at a total energy of $E=0.1$ eV. The intervals that correspond to excitation, ionization, and exchange are marked.

the ratio of nuclear charge to wing particle charge is less than one ($Z/q < 1$) the deflection function can become, in a suitable energy range, nonmonotonic. We shall return to this observation later. The normalization above holds whether or not the deflection function is monotonic.

Over the energy range we use to calculate the threshold exponent the deflection function stays monotonic in the ionization interval. Because only one trajectory contributes to a final projectile energy ε, the sum of Eq. (5) has only one term remaining with the consequence that the semiclassical result collapses to the classical cross section, without any effects from the phase factor of Eq. (6), giving

$$P_{\varepsilon,\varepsilon'} = \mathcal{P}(\varepsilon,\varepsilon') \equiv \frac{1}{R}\left|\frac{\partial r'}{\partial \varepsilon}\right|_{\varepsilon'}. \qquad (7)$$

The total cross section is proportional to the intervals of r' (which can be read off from the deflection function) for which a certain process occurs. For ionization the cross section is

$$P_{\text{ion}}(E) = \frac{1}{R}\int_0^E \left|\frac{\partial r'}{\partial \varepsilon}\right|_{\varepsilon'} d\varepsilon = \frac{1}{R}\int_{r' \in \text{ion}} dr' = \frac{\Delta r'(\text{ion})}{R}. \qquad (8)$$

III. RESULTS

When $Z=1/4$ and the bound electron is in its ground state the total ionization cross section for electron impact (Fig. 2) does not show an obvious power-law structure. Between 0.01 eV, which is the lowest energy for which the cross section is obtained, and 0.08 eV the calculated points are better fitted to an exponential law of the form $A\exp(-\lambda/\sqrt{E})$. Our best-fit value for A was 0.6430 and for λ it was 0.3056. We used a Runge-Kutta-Merson method for the numerical integration and set the accuracy to ten decimal
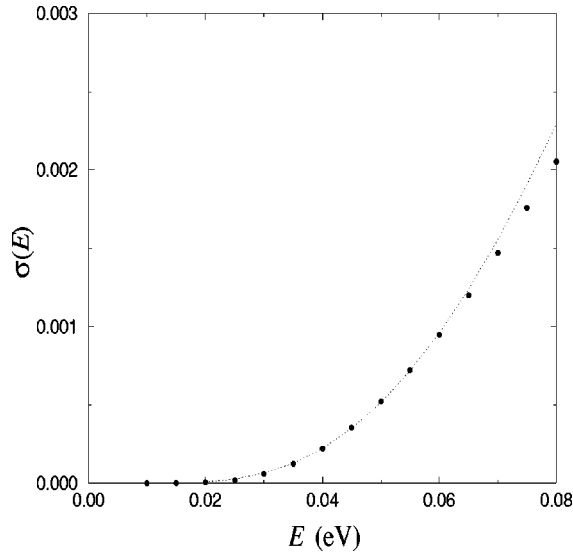
FIG. 2. Total ionization cross section for electron impact on a nucleus with charge $Z=1/4$ and a bound electron with energy $\varepsilon' = -Z^2/2n^2$, where $n=1$. The filled circles are the calculated values and the line is $A \exp(-\lambda/\sqrt{E})$, with $A=0.6430$ and $\lambda=0.3056$.

places. Even at the very low energy of 0.08 eV the calculated cross section deviates away from the fitted line. If the cross section is continued to higher energies (Fig. 3), it is found to become less steep and reach a maximum at approximately 0.2 eV, at which point it begins to decrease.

In the purely classical work of Dimitrijević *et al.* [6] using classical trajectory Monte Carlo calculations in three dimensions, a threshold law of the form $A \exp(-\lambda/\sqrt{E})$ is also found. For the full-collision treatment values of $A = 1.875\,67\times10^3$ and $\lambda=0.330\,698$ were obtained. The values for λ compare favorably (the values for A are not the same because of the different ways that the cross section has been calculated). It is found in [6] that inclusion of another point at $E=0.1088$ eV resulted in a much worse fit. We see now that the slope of the cross section lessens at this energy (Fig. 3), so we are able to explain this fact. Ionization inter-
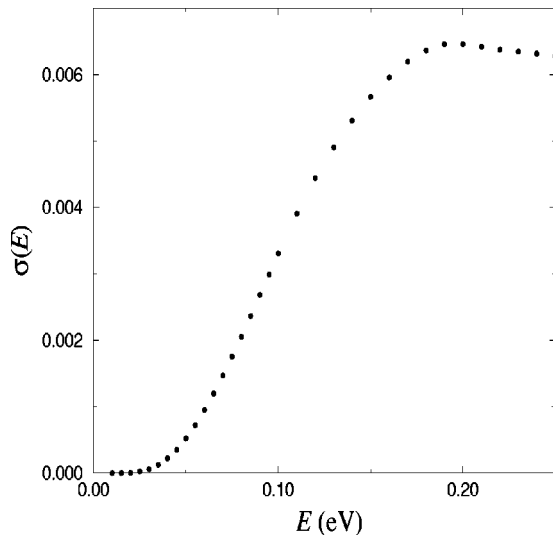

FIG. 3. Total ionization cross section of Fig. 2 plotted between $E=0$ and 0.2 eV.
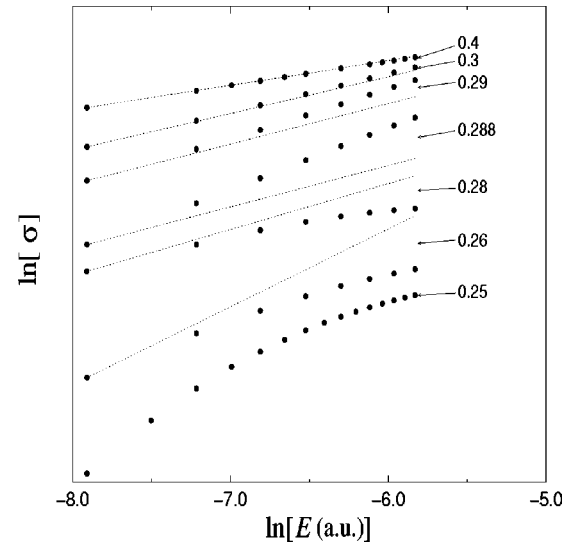

FIG. 4. Ionization cross sections plotted on a log-log graph for various values of Z. Circles correspond to calculated values and the lines are the power law (1) with exponent (2). The cross sections are shifted for clarity.

vals were found to disappear below an energy of 0.0653 eV. Such an effect might be an artifact of their calculations and was not found here.

An exponential threshold law was also obtained in a recent analytical semiclassical treatment [7] that is based on a half-collision approach. The analytical threshold law derived was in very good agreement with the numerical classical Monte Carlo calculations [6]. The S-matrix theory employed in this work is a more rigourous treatment in the sense that it probes the sensitivity of the cross section on the initial state. The full-collision S-matrix approach confirms the functional behavior predicted by the half-collision approach.

Even though the threshold exponent (2) becomes infinite when $Z/q=1/4$, Wannier theory still predicts a power law for the ionization cross section for all $Z/q>1/4$. This prediction was tested by plotting the cross section between 0.01 and 0.08 eV on a logarithmic scale graph (Fig. 4).

A power law would give a straight line on this graph. Rather than an abrupt change from an exponential law to a power law occurring at $Z=0.25$ as would be expected from Wannier theory (which is based on the saddle dynamics only), the threshold behavior changes smoothly from an exponential behavior at $Z=0.25$ to what looks like behavior that will give the expected power law at about $Z=0.2865$. The behavior then again becomes different from a power law (at this point the ionizing trajectories cross the $r_1=r_2$ diagonal), but quickly converges to a power law with the Wannier exponent (2) when $Z>0.3$.

Even when a power law is not apparent it cannot be excluded that the power-law behavior predicted by Wannier theory holds for even lower energies. Rather the cross section displays behavior of a different form for the calculated points (>0.01 eV), which may not be the case as $E\to0$. Numerical constraints meant that energies below 0.01 eV could not be accurately studied.

A. Characteristics of the deflection function

Cross sections are produced by extracting the ionization interval from the systems corresponding deflection function.
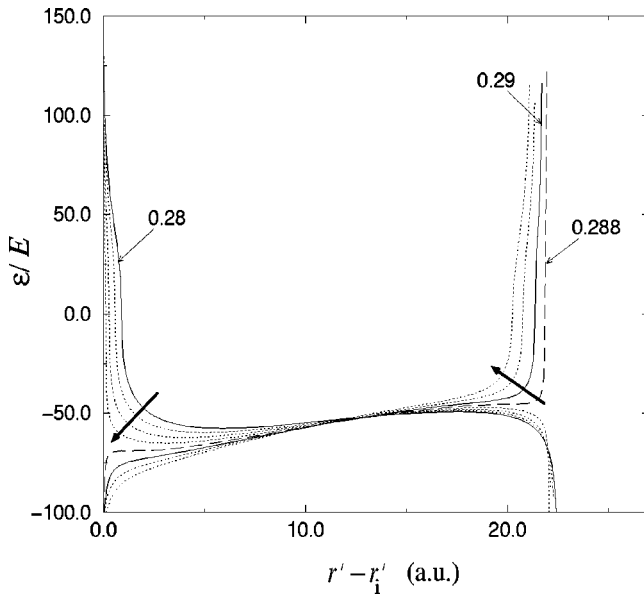
FIG. 5. Deflection functions at $E=0.02$ eV for values of Z between 0.28 and 0.294. Each subsequent deflection function in the direction of the bold arrows corresponds to an increase in Z of 0.002. r_i' is the initial value of r' for each deflection function.

The deflection functions were found to display some interesting properties. When they are plotted for different values of Z at $E=0.02$ eV (Fig. 5) the most noticeable effect is that for values of Z whose cross sections display a clear power law the deflection functions are "flipped." The excitation interval is on the right rather than the left. Another interesting feature is that the deflection functions on this plot for $0.28 \leqslant Z < 0.288$ are nonmonotonic within the exchange scattering interval with the possibility of three trajectories contributing to the same final energy for the initially incoming electron. In general, the deflection function $\varepsilon(r')$ can, under suitable conditions, become nonmonotonic when $Z/q < 1$. Usually this occurs at very low energy; however, as the charge ratio decreases the energy at which this can happen increases. Figure 5 shows a nonmonotonic deflection function at $Z=0.286$ for $E=0.02$ eV.

For the particular case of $q=1$ and $Z=1/4$ we see that the nonmonotonicity is apparent at energies $E=0.3$ eV (Fig. 6). When $Z=0.24$ the deflection function (which is not plotted) displays a different form of nonmonotonicity; it is now continuous, oscillating between two positive values, i.e., only excitation can occur and only between two energies.

When we plot (Fig. 7) the three trajectories that contribute to $\varepsilon/E=3.125 \times 10^{-2}$ a.u./0.3 eV $(\varepsilon = -Z^2/2)$ we can see quite clearly the way the trajectories have been affected by the potential. More than one trajectory contributes to a final projectile energy ε so there will be an effect from the phase factor in Eq. (5).

The deflection function for one particular Z also changes in a similar manner to Fig. 5 when the energy is increased (as opposed to increasing Z at constant E). So calculating a cross section could, in practice, involve the use of different types of deflection function. At the point where a flip occurs the slope through the ionization interval is very steep indeed. We were unable to calculate a cross section with any reli-
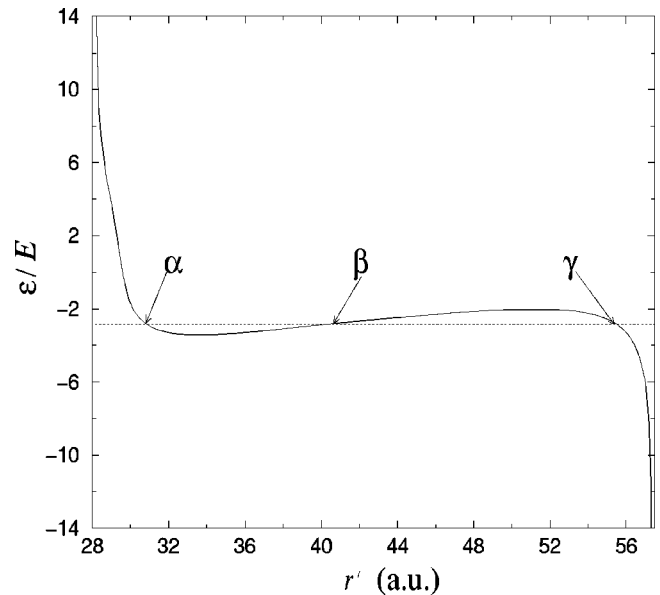

FIG. 6. Classical deflection function at a total energy of $E=0.3$ eV, which displays nonmonotonic behavior. α, β, and γ mark different trajectories that lead to the same final energy for the projectile electron (ground-state energy for the hydrogenic atom with charge $Z=1/4$).

ability for these types of deflection function, hence the absence of cross sections between $Z=0.28$ and 0.288 in Fig. 4.

B. Ionizing trajectories

Ionizing trajectories plotted over a contour plot of the potential surface are presented in Figs. 8–11. In Fig. 8, $Z=0.4$ and the cross section for this system follows very closely a power law with the Wannier exponent. Two ionizing trajectories are plotted, one with a total energy $E=0.03$ eV and the other with $E=0.07$ eV. The trajectories follow very similar paths and move out onto and along the ridge almost indistinguishably. These types of trajectories corre-
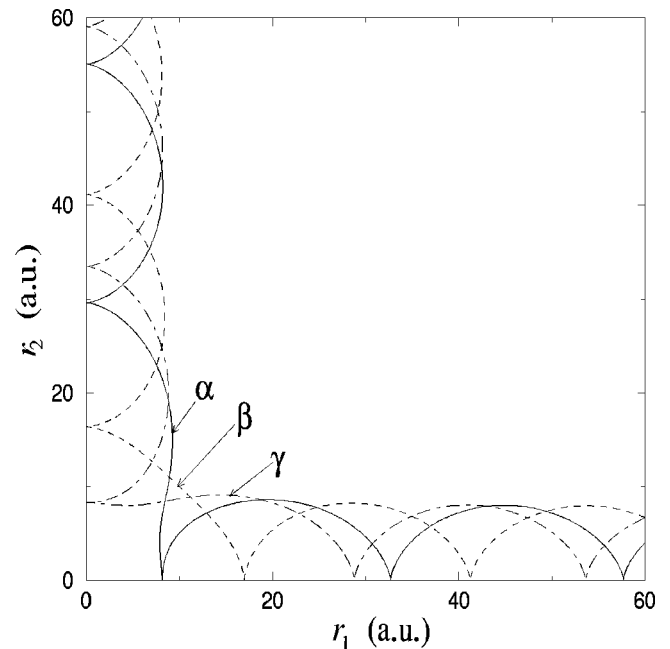

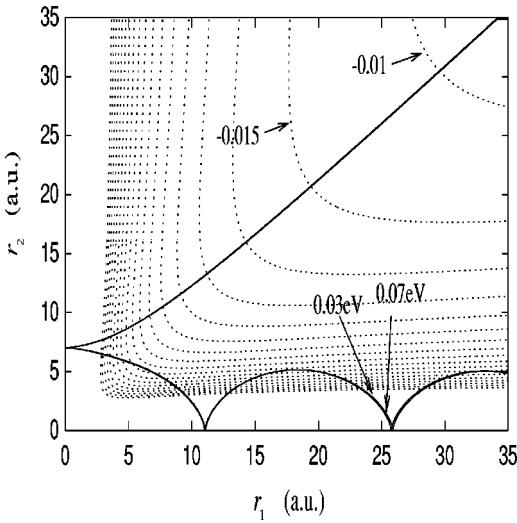FIG. 7. Trajectories corresponding to α, β, and γ in Fig. 6.

FIG. 8. Contour plot of the potential for $Z=0.4$. The contour plot begins at r_i ($i=1,2$)≈ 2 to allow incremental contours without too much bunching. Trajectories leading to ionization with equal energy sharing between the electrons ($\varepsilon/E=0.5$) are plotted for different values of total energy E.

spond to the orbits that Wannier observed [1] that do not differ in the reaction and Coulomb zones when they have zero energy or small energy. All trajectories that led to double escape at zero energy will continue to do so at finite energy; however, other trajectories leading to double escape will also be possible because the energy is finite. This is in agreement with Wannier and for cases like this Wannier theory is valid.

Figure 9 is for the $Z=0.25$ case where the cross section follows an exponential law. There is no longer such a simple
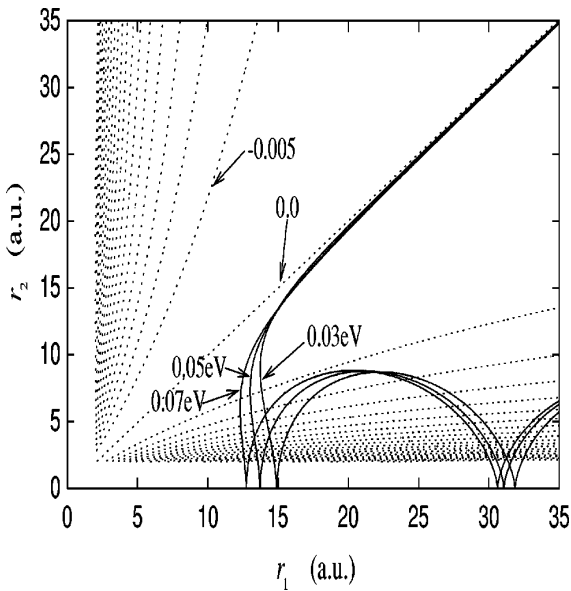

FIG. 9. Contour plot of potential and ionization trajectories for $Z=0.25$.

relationship between higher energies and more orbits leading to double escape. Because the trajectories begin to move out along the ridge at different positions they are affected by the
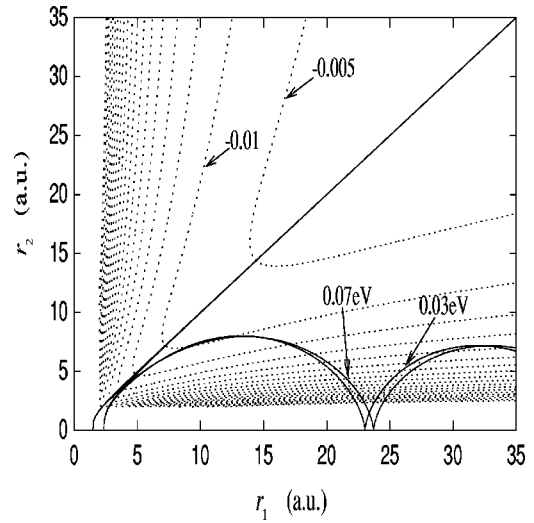

FIG. 10. Contour plot of potential and ionization trajectories for $Z=0.286$.

potential in different ways. Ultimately the potential tends to ''focus'' trajectories with different energies to different extents, pulling them onto the ridge. The effect of the potential is no longer uniform (as it is when the trajectories are nearly identical).

Figure 10 shows ionizing trajectories that clearly differ from each other (although this difference is not great). They are plotted for the case when $Z=0.286$. Figure 4 shows the cross section flattening out as Z increases from 0.25. At $Z=0.2865$ it would be logical to extrapolate this evolution to a cross section that was near the expected power law. The difference in trajectories in this plot is less than the $Z=0.25$ case, so a threshold law closer to that predicted by Wannier is not unreasonable.

In Fig. 11, $Z=0.288$ and the trajectories have crossed the $r_1=r_2$ diagonal and clearly follow different paths. The difference is greater than the previous plot and the cross section also differs from the Wannier power law to a greater extent.
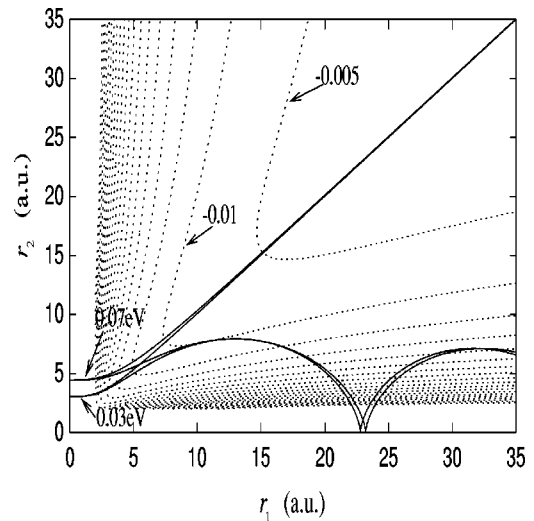

FIG. 11. Contour plot of potential and ionization trajectories for $Z=0.288$.

IV. CONCLUSION

Using semiclassical S-matrix theory for electron-impact ionization of an atom of nuclear charge Z we have studied the form of the cross section as Z approaches 1/4, at which point the Wannier exponent diverges. The cross section has been found not to follow a power law for a range of values of Z and E. It cannot be stated categorically, however, that the cross section does not follow a power law at energies lower than those studied. At the point where the Wannier exponent diverges ($Z=1/4$) the cross section is best fitted by an exponential function. The coefficient of this function agrees well with that calculated in the full-collision purely classical treatment [6]. This S-matrix approach confirms the functional behavior obtained in a recent analytical semiclassical treatment [7]. In the Coulombic system studied we have demonstrated the existence of interference effects with the possibility of more than one trajectory contributing to the same final state so that the semi-classical S matrix must be summed coherently.

It has been shown that when ionizing trajectories for different low energies are indistinguishable a power law with the Wannier exponent is obtained. Systems where the ionizing trajectories are different give rise to behavior that at the low energies studied here does not follow a power law. The dynamics within the near zone can become crucial, particularly where interference is observed. Semiclassical S-matrix theory incorporates the exact potential and includes all behavior within the near zone. These additions give rise to a threshold cross section that differs from that predicted by Wannier theory.

Since different threshold laws are obtained because trajectories follow different paths for different energies we question whether at very low energies (much less than 0.01 eV) and for a very short energy range the threshold law calculated would coincide with the Wannier law. At these energies and for this small range the trajectories would be indistinguishable and it would seem, objectively, that the Wannier law should be regained. Figure 4 shows that at lower energies for systems that do not give a power law the cross section has a slope that gets closer to that calculated using the Wannier exponent. Due to numerical constraints the region of very low energy could not be studied with confidence.

APPENDIX: REGULARIZATION OF THE COULOMB SINGULARITIES

We can regularize two of the three possible binary collisions ($r_1=0$, $r_2=0$) in the Hamiltonian (4) by introducing a point transformation to oscillatorlike coordinates where $r_i = Q_i^2$. The conjugate momenta are $p_i = P_i/2Q_i$, where P_i are the new momenta that remain finite at $r_i=0$. So that the singularity is passed in small time steps with respect to real time, the time variable is changed to become $d\tau = r_1 r_2/(r_1 + r_2)dt$. We work with a Hamiltonian of zero value to keep the form of Hamilton's equations invariant under the time-variable transformation. The regularized, singularity free Hamiltonian reads

$$\mathcal{H} = \frac{P_1^2 Q_2^2}{8} + \frac{P_2^2 Q_1^2}{8} - Z(Q_1^2 + Q_2^2) + Q_1^2 Q_2^2 \left[\frac{1}{Q_1^2 + Q_2^2} - E \right].$$

(A1)

[1] G. H. Wannier, Phys. Rev. **90**, 817 (1953).
[2] J.-M. Rost, Phys. Rev. Lett. **72**, 1998 (1994).
[3] J.-M. Rost, J. Phys. B **28**, 3003 (1995).
[4] H. Klar, J. Phys. B **14**, 3255 (1981).
[5] J. M. Feagin, J. Phys. B **17**, 2433 (1984).
[6] M. S. Dimitrijević, P. V. Grujić, and N. S. Simonović, J. Phys. B **27**, 5717 (1994).
[7] W. Ihra, F. Mota-Furtado, and P. F. O'Mahony, Phys. Rev. A **55**, 4263 (1997).